

Measuring Exoplanetary Radii Using Transit Photometry

Sarah Tang¹, William Waalkes²

¹Fairview High School, Boulder, Colorado

²University of Colorado, Boulder, Colorado

ABSTRACT

The goal of this study was to measure the radii and constrain the orbital periods of three hot Jupiter exoplanets: HAT-P-25b, HAT-P-9b, and HAT-P-30b. Raw images of the host stars were acquired from the Apache Point Observatory in New Mexico. A data processing pipeline utilizing the Python programming language was used to convert the raw data images into calibrated pixels and transit light curve graphs. The graphs of HAT-P-25b and HAT-P-30b were fit with multiple light curve models, which varied based on a given range of radius and time of mid-transit parameters within the code. The data of HAT-P-9b were not further analyzed due to a non-detection in the data. We hypothesized that the differences between the dates the exoplanets were discovered and the dates on which we observed them have no effect on the radii of the exoplanets and their times of mid-transit. Chi-square Goodness of Fit tests were performed on all light curve models to isolate the chi-square value closest to 1.0. Chi-square maps were used to estimate the 1σ error bars for all light curve calculations. A significant shift in mid-transit time (-0.41 ± 0.31 hours from expected value) was detected for HAT-P-25, and a significant difference (0.04 ± 0.0020) from the literature value was calculated for the normalized radius (R_p/R_*) of HAT-P-30b. These findings stress the importance of updating exoplanetary measurements and will help scientists obtain more accurate knowledge about the characteristics of these exoplanets and their evolution over time.

INTRODUCTION

Exoplanets are planets that orbit a star other than the Sun (1). The study of exoplanets enables increased understanding about the formation of planets, interactions between planets, and how Earth's solar system differs from other solar systems (2).

Many detection methods exist to help discover these exoplanets; one such method is known as the transit detection method. Since planets orbit their host stars in consistent time frames, they can be detected through planetary transits, which occur when a planet crosses the disk of its host star. From the observer's viewpoint, the exoplanetary transit causes a dimming in the detected amount of light emitted from the host star (3). This change in stellar flux is analyzed

through the process of photometry (light measurement) to determine whether a planet is transiting or not. The transit detection method is the only exoplanet detection method that can measure the radius of the given exoplanet, making it a highly valuable and efficient approach (4).

Moreover, the recent development of new technologies and equipment has allowed for further exploration and discovery of exoplanets specifically using the transit detection method. A clear example of this advancement was the Kepler Mission, launched in 2009 by the National Aeronautics and Space Administration. This mission aimed to detect exoplanets specifically using the transit photometry method. By 2015, Kepler had detected 1030 exoplanets (5).

In this study, we analyzed the transit light curves of three exoplanets: HAT-P-25b, HAT-P-9b, and HAT-P-30b, to measure their radii and constrain their orbital periods to analyze if and how these planets have changed since their discovery. HAT-P-25b, HAT-P-9b, and HAT-P-30b are all hot Jupiter exoplanets, which are defined as gas giants with orbital periods of ten days or less. We hypothesized that the differences between the dates the exoplanets were discovered and the dates on which we observed them would have no effect on the radius and time of mid-transit parameters of the exoplanets. To test this hypothesis, we compared our calculated values to the previously published literature values for the radius and time of mid-transit parameters of each exoplanet observed: HAT-P-25b, HAT-P-9b, and HAT-P-30b (6-8). The literature values for each planet were obtained in 2010, 2009, and 2011, respectively (6-8).

The overarching goal of our research was to gain information regarding how exoplanets change over time and how these exoplanets compare to the planets within the Earth's solar system through the analysis of exoplanet characteristics. The results from this study would increase the understanding of planetary characteristics in general, and may provide information on how the parameters of planets in the Earth's solar system are projected to change in the near and far future. We focus on the radii and orbital periods of exoplanets because these measurements are used in many equations that calculate other planetary characteristics, such as mass and density. Furthermore, the study of exoplanets is a relatively new field, and limited follow-up analysis has been performed on the exoplanets already detected and confirmed. Research regarding follow-up studies on exoplanets is critical for ensuring that we are obtaining accurate data regarding

general planetary characteristics, so that in a larger sense, we can meticulously study planetary populations.

RESULTS

Light Curve Analysis

To study the transit light curve graphs of HAT-P-25b and HAT-P-30b in terms of relative light flux, the graphs were normalized to a baseline value of one. We were able to calculate the normalized radii of both planets using the following transit depth equation:

where ΔF is the observed change in flux, F is the stellar flux, R_p is the radius of the planet, and R_* is the radius of the star that hosts the planet.

$$\text{Equation 1} \quad \frac{\Delta F}{F} = \frac{R_p^2}{R_*^2}$$

Our results do not support our hypothesis because the values that we detected for the time of mid-transit of HAT-P-25b and the radius of HAT-P-30b (calculated to be 0.15 ± 0.02) differed from the literature values with statistical significance. For HAT-P-25b, we found the normalized radius to be 0.13 ± 0.03 , which is consistent with the literature value of 0.1275 ± 0.0024 (Table 1). However, the mid-transit time we found for HAT-P-25b was shifted -0.41 ± 0.31 hours from the expected value (Figure 1a). Our calculated mid-transit time significantly differs from the expected mid-transit time of 0 by more than the 1σ error bar value (Figure 2a). The 1σ error bar values for our light curve measurements were determined through chi-squared maps, which are visualizations of the 1σ error bar region of a measurement.

TABLE 1 HAT-P-25b		
Parameter	Calculated Value	Literature Value
Normalized Planetary Radius (R_p/R_*)	0.13 ± 0.030	0.13 ± 0.002
Mid-transit Time (hours from expected value)	-0.41 ± 0.310	
Orbital Period (days)		3.65 ± 0.00002

Table 1. Measured results and the corresponding literature values for the normalized planetary radius (R_p/R_*), time of expected mid-transit (hours), and orbital period (days) of HAT-P-25b.

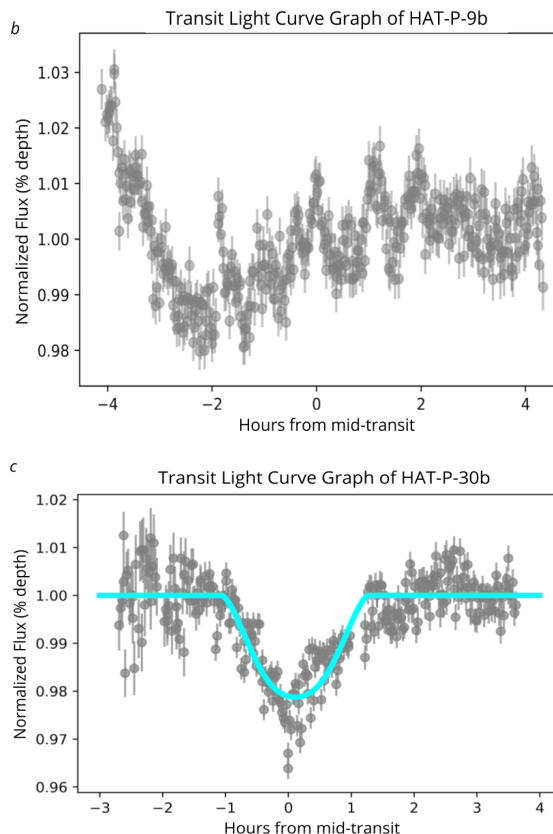
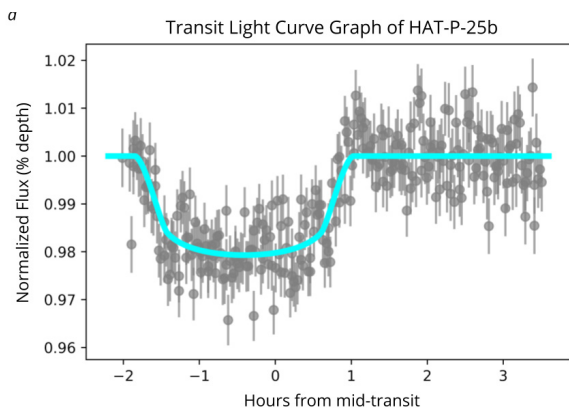


Figure 1. Normalized transit light curve graphs for the planets (a) HAT-P-25b, (b) HAT-P-9b, and (c) HAT-P-30b. These transit light curve graphs have been modeled with a best-fit transit light curve.

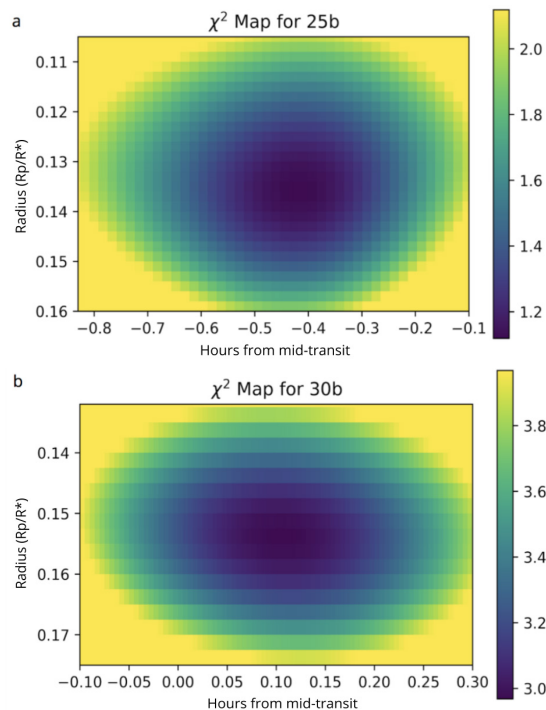


Figure 2. Chi-square maps for the calculated values of (a) HAT-P-25b and (b) HAT-P-30b. The 1σ error bar range is shown in purple, blue, and green.

The expected mid-transit time is 0 because the best-fit model for our transit light curve is based on the orbital period stated in the literature (6). Basing our light curve model on this existing parameter, comparisons can be made between our measurements and the literature values, namely in regards to the mid-transit time of the exoplanet. This detected shift for HAT-P-25b indicates that the orbital period of this planet can be constrained further with future analysis.

For HAT-P-30b, the normalized planetary radius was calculated using equation 1 to be $0.15 \pm 0.02 R_p/R_*$. This value significantly differs from the literature result by a value of $0.04 \pm 0.0020 R_p/R_*$ (Table 2) (8). This signifies that the radius of this planet can be constrained further. As for the time of mid-transit, we detected a value of 0.11 ± 0.20 hours from the expected time, and since the expected mid-transit time of 0 falls within the 1σ error bar values of our results, we can conclude that the period of this planet is robust and consistent (Figure 1c).

Parameter	Calculated Value	Literature Value
Normalized Planetary Radius (R_p/R_*)	0.15 ± 0.020	0.11 ± 0.002
Mid-transit Time (hours from expected value)	0.11 ± 0.200	
Orbital Period (days)		2.81 ± 0.000005

Table 2. Measured results and the corresponding literature values for the normalized planetary radius (R_p/R_*), time of expected mid-transit (hours), and orbital period (days) of HAT-P-30b.

DISCUSSION

In this study, we detected a significant shift from the literature value in the mid-transit time of the hot Jupiter exoplanet, HAT-P-25b (6). This information will be helpful to more accurately predict the transit times for this planet in the near future. HAT-P-25b was discovered in 2010, and since our plots are modeled on the parameters found at that time, our study signifies that the time of mid-transit has shifted by -0.41 hours in the past 8 years, and approximately 3.1 minutes every year. This means that the center of this transit occurred approximately 24 minutes earlier than expected.

It is important to keep information about planetary periods updated to actively study and keep track of these planets. The importance of this detected change in the time of mid-transit is demonstrated by the fact that in 20 years, HAT-P-25b will transit more than one hour earlier than the expected time. This is a substantial amount of time when observing planets.

Furthermore, the shift in the mid-transit time of HAT-P-25b implies that the orbital period of this exoplanet has shifted from $3.652836 \text{ days} \pm 0.000019 \text{ days}$, as stated in the literature, to around $3.653 \text{ days} \pm 0.017 \text{ days}$ (6). However, the actual constraint of the orbital period of HAT-P-25b cannot be determined until additional data is collected of a current span of continuous transits of HAT-P-25b.

The significant difference that was detected for the normalized radius of HAT-P-30b ($0.04 \pm 0.0020 R_p/R_*$) can be used to more accurately constrain the radius of this planet for more precise measurements. No significant difference was found for the mid-transit time of this planet compared to literature results found in 2011 (8). This signifies that the orbital period of this planet is consistent and unfluctuating.

These detected differences may be the result of instrumentation factors or slight dissimilarities to the instrumentation techniques used by the mission that initially detected these exoplanets. Alternatively, these results may have occurred from the existence of true planetary characteristic changes, although this conclusion cannot be drawn until more data concerning these exoplanets are analyzed.

Since our hypothesis was not supported by our data, and statistically significant differences were found for the time of mid-transit of HAT-P-25b and the radius of HAT-P-30b, we can conclude that these characteristics can be constrained with further analysis. These results also stress the importance of updating exoplanetary characteristics' measurements for the accurate study of planetary populations and solar systems as a whole. Overall, these findings will encourage and allow scientists to obtain more accurate knowledge about these exoplanets and their characteristics.

METHODS

In the Kepler Mission, the Kepler Data Processing Pipeline was used to convert raw photos taken from a telescope and camera into calibrated pixels and transit graphs. The stages in the Kepler Pipeline include data acquisition, calibration, photometry, presearch data conditioning, transiting planet search, and data validation (9). In our study, we used a data processing pipeline with similar stages to the Kepler Pipeline: data acquisition, calibration, photometry, light curve modeling, and light curve analysis.

Data Acquisition

We used the 0.5 meter Astrophysical Research Consortium Small Aperture Telescope (ARCSAT) and Flare Camera imaging instrument located in Sunspot, New Mexico, during the nights of January 16, 17, and 18 of 2018 to collect the data. We used these instruments through remote observing on a computer. The three planets we observed (HAT-P-25b, HAT-P-9b, and HAT-P-30b) are all hot Jupiter exoplanets, therefore, we used the R filter on the Flare Camera because these types of planets and their host stars tend to emit wavelengths of light between 550 and 800 nanometers (10-11). This filter was used to produce the most accurate images possible for the given target host stars.

Calibration

Using the ARCSAT telescope and the Flare Camera imaging instrument, we acquired four types of images: raw data science images, bias images, dark images, and domeflat

images. The raw data science images were taken of the target star and neighboring comparison stars. Bias images are short exposures taken with the camera cover on to block out any light exposure. Dark images are bias images with shorter frame times, that specifically correct for the amount of accumulated electrons currently present on the Charge-Coupled Device (CCD) detector. Both dark and bias images reduce CCD flaws and increase signal-to-noise ratio of the data to obtain the highest amount of accuracy. Domeflat images are 60 second exposures taken of the inside of the observatory dome for consistency. These images reduce pixel sensitivity variations within the CCD (12).

Using these bias, dark, and domeflat images, we created the Masterbias, Masterdark, and Masterflat images. To create these Masterimages, all images of that specified image type were stacked and averaged using the Python programming language. Equation 2 was then used to obtain the final calibrated images:

$$\text{Equation 2} \quad \frac{(\text{Raw Science} - \text{MasterDark})}{(\text{Masterflat} - \text{Masterbias})}$$

These calculations were completed using the Python programming language.

Photometry

We used a graphical user interface titled AstrolmageJ to stack all of the final calibrated image files to perform aperture photometry (light measurement within a fixed size) on the target star and three neighboring comparison stars (13). These light measurements of the target and comparison stars were then normalized and converted into numerical values of light flux. These values of relative light flux for each image were stored in text files along with their corresponding 1σ error bar values (generated by AstrolmageJ) and barycentric Julian date, which is the time that the image was taken.

Light Curve Modeling

For each observed exoplanet, we used the timestamp and light flux value (as generated by AstrolmageJ) of the target star from each image to generate the transit light curve graphs of HAT-P-25b (**Figure 1a**), HAT-P-9b (**Figure 1b**), and HAT-P-30 (**Figure 1c**), with hours from mid-transit on the x-axis and normalized flux on the y-axis. These graphs were created through the Python programming language. Then, to study the transit light curves in terms of relative light flux and transit depth, we fit a line to the baseline flux of the transit light curve graph and normalized that baseline value to a value of one.

However, the data collected for HAT-P-9b were not analyzed further because there is a non-detection in the data, which could be due to instrumentation or Charge-Coupled Device errors.

The BATMAN Python package was used to fit multiple light curve models to the HAT-P-25b and HAT-P-30b normalized transit light curve graphs (14). These models were varying

based on a given range of values for the radius and time of mid-transit parameters within the code. Chi-squared goodness of fit tests were performed on each light curve model to find the chi-squared value closest to 1.0, which would signify a strong data to model fitting. We found the reduced chi-square values for HAT-P-25b and HAT-P-30b to be 1.1 (**Figure 2a**) and 2.9 (**Figure 2b**), respectively.

ACKNOWLEDGMENTS

We would like to thank Dr. Paul Strode (Department of Biology, Fairview High School) for providing guidance and support, and teaching me about the nature of science.

Received: November 28, 2018

Accepted: April 18, 2019

Published: May 7, 2019

REFERENCES

1. Fridlund, Malcolm, et al. "The way forward." *Astrophysical Journal*, vol. 205, no. 4, (2016): pp. 349-372., doi:10.1007/s11214-016-0247-2.
2. Carson, Joseph, et al. "Why Study Exoplanets?". College of Charleston, (2013): www.exoplanets.cofc.edu/why.html.
3. Clampin, M., et al. "Detection of Planetary Transits with the James Webb Space Telescope." *European Space Agency*, (2007): www.sci.esa.int/jwst/47523-clampin-m-et-al-2007/#.
4. Braun, Kaspar von, et al. "Searching for Planetary Transits in Galactic Open Clusters." *Astronomical Society of the Pacific*, vol. 117, no. 828, (2005): pp. 141-159., doi:10.1086/427982.
5. Soutter, Jack, et al. "The Kilodegree Extremely Little Telescope: Searching for Transiting Exoplanets in the Northern and Southern Sky." *Australian Space Research Conference*, (2015): www.researchgate.net/publication/302569516.
6. Quinn, S.N., et al. "HAT-P-25b: a Hot-Jupiter Transiting a Moderately Faint G Star." *The Astrophysical Journal*, vol. 745, no. 1, (2011): pp. 80-89., doi:10.1088/0004-637X/745/1/80.
7. Shporer, Avi, et al. "HAT-P-9b: A Low Density Planet Transiting a Moderately Faint F star." *The Astrophysical Journal*, vol. 690, no. 2, (2008): pp. 1393-1400., doi:10.1088/0004-637X/690/2/1393.
8. Johnson, John Asher, et al. "HAT-P-30b: A Transiting Hot Jupiter on a highly oblique orbit." *The Astrophysical Journal*, vol. 735, no. 1, (2011): pp. 24-31., doi:10.1088/0004-637X/735/1/24.
9. Tenenbaum, Peter, et al. "Detection of Transiting Planet Candidates in Kepler Mission Data." *National Aeronautics and Space Administration*, (2012): www-conf.slac.stanford.edu/statisticalissues2012.
10. Wang, Ji, et al. "On the Occurrence Rate of Hot Jupiters in Different Stellar Environments." *The Astrophysical Journal*,

vol. 799, no. 2, (2009): pp. 229-237., doi:10.1088/0004-637X/799/2/229.

11. Hawley, Suzanne, et al. "ARCSAT." New Mexico State University, (2014): www.apo.nmsu.edu/Telescopes/ARCSAT/index.html.
12. "The Types of Images." *Raw Astrophotography Data*, www.rawastrodata.com/pages/typesofimages.html.
13. Collins, Karen A., et al. "AstroImageJ: Image Processing and Photometric Extraction for Ultra-Precise Astronomical Light Curves (Expanded Edition)." *AstroImageJ: ImageJ for Astronomy*, (2017): www.astro.louisville.edu/software/astroimagej.
14. Kreidberg, Laura. "batman: BAsic Transit Model cAlculationN in Python." *Publications of the Astronomical Society of the Pacific*, vol. 127, (2015): pp. 1161-1165., www.cfa.harvard.edu/~lkreidberg/batman.

Copyright: © 2019 Tang and Waalkes. All JEI articles are distributed under the attribution non-commercial, no derivative license (<http://creativecommons.org/licenses/by-nc-nd/3.0/>). This means that anyone is free to share, copy and distribute an unaltered article for non-commercial purposes provided the original author and source is credited.